

# Differential Mechanisms of Binding of Anti-Sigma Factors *Escherichia coli* Rsd and Bacteriophage T4 AsiA to *E. coli* RNA Polymerase Lead to Diverse Physiological Consequences<sup>∇</sup>

Umender K. Sharma<sup>1,2,\*</sup> and Dipankar Chatterji<sup>2</sup>

*AstraZeneca Research and Development, Bellary Road, Hebbal, Bangalore, India,<sup>1</sup> and Molecular Biophysics Unit, Indian Institute of Science, Bangalore, India<sup>2</sup>*

Received 13 November 2007/Accepted 12 March 2008

**Anti-sigma factors *Escherichia coli* Rsd and bacteriophage T4 AsiA bind to the essential housekeeping sigma factor,  $\sigma^{70}$ , of *E. coli*. Though both factors are known to interact with the C-terminal region of  $\sigma^{70}$ , the physiological consequences of these interactions are very different. This study was undertaken for the purpose of deciphering the mechanisms by which *E. coli* Rsd and bacteriophage T4 AsiA inhibit or modulate the activity of *E. coli* RNA polymerase, which leads to the inhibition of *E. coli* cell growth to different amounts. It was found that AsiA is the more potent inhibitor of in vivo transcription and thus causes higher inhibition of *E. coli* cell growth. Measurements of affinity constants by surface plasmon resonance experiments showed that Rsd and AsiA bind to  $\sigma^{70}$  with similar affinity. Data obtained from in vivo and in vitro binding experiments clearly demonstrated that the major difference between AsiA and Rsd is the ability of AsiA to form a stable ternary complex with RNA polymerase. The binding patterns of AsiA and Rsd with  $\sigma^{70}$  studied by using the yeast two-hybrid system revealed that region 4 of  $\sigma^{70}$  is involved in binding to both of these anti-sigma factors; however, Rsd interacts with other regions of  $\sigma^{70}$  as well. Taken together, these results suggest that the higher inhibition of *E. coli* growth by AsiA expression is probably due to the ability of the AsiA protein to trap the holoenzyme RNA polymerase rather than its higher binding affinity to  $\sigma^{70}$ .**

Anti-sigma proteins play an important role in regulating gene expression in bacteria. A number of anti-sigma factors have been reported in the literature (for reviews, see references 4, 14, and 15). A majority of the known anti-sigma factors bind to alternate sigma factors and thus bring about changes in transcription profiles and help the organisms to adapt to new environmental conditions. Bacteriophage T4 AsiA and *Escherichia coli* Rsd are two anti-sigma factors that bind to the housekeeping sigma factor  $\sigma^{70}$  of *E. coli*. AsiA is a 10-kDa protein (3, 23) which, in addition to acting as an anti-sigma factor, also acts as a positive activator of T4 middle gene transcription (24). However, the expression of AsiA in *E. coli* results in the inhibition of transcription, which leads to the inhibition of cell growth. The other anti-sigma factor, *E. coli* Rsd, was identified by Jishage and Ishihama (17) as a stationary-phase protein. It has been proposed that by sequestering  $\sigma^{70}$  of *E. coli*, this protein promotes the transcription of stationary-phase genes by favoring the association of core RNA polymerase (RNAP) with  $\sigma^{38}$  of *E. coli* (17, 22). It has also been shown that purified Rsd inhibits the in vitro transcription from selected *E. coli* promoters to various degrees (17).

Both AsiA and Rsd have been shown to interact with region 4 of  $\sigma^{70}$ . Nuclear magnetic resonance studies (19) and analyses of the in vivo interaction of AsiA with truncated  $\sigma^{70}$  fragments (29) have shown that both region 4.1 and 4.2 are involved in this interaction. Initial studies of Rsd binding to *E. coli*  $\sigma^{70}$  had suggested that this interaction is limited to region 4.2 (18), but

subsequent studies found that region 4.1 is also involved in the interaction (12, 26, 33). Electrospray ionization mass spectrometry analysis (16) showed that in addition to binding to  $\sigma^{70}$ , Rsd could also associate with core RNAP. Pineda et al. (26), using the bacterial two-hybrid system, in vitro transcription assays, and bioinformatics analysis, concluded that AsiA and Rsd belong to the same family of proteins and have similar mechanisms of action. However, the very recently reported crystal structure of the Rsd- $\sigma^{70}$  complex does not support this view (25).

Since  $\sigma^{70}$  activity is essential for growth and survival of *E. coli*, inhibition of this sigma factor is expected to be lethal. As both Rsd and AsiA bind to  $\sigma^{70}$ , we were interested in analyzing the effects of expression of these anti-sigma factors on in vivo transcription and growth of *E. coli*. To understand the molecular basis of their differential inhibitory properties, we studied the mechanisms of interaction of these two anti-sigma factors, with  $\sigma^{70}$  and holoenzyme (holo) RNAP. In addition, we estimated their affinities of binding to  $\sigma^{70}$ . We propose that because of differences in their mechanisms of binding to RNAP, these proteins can modulate the inhibition of transcription to different levels inside the *E. coli* cell.

## MATERIALS AND METHODS

**Bacterial and *Saccharomyces cerevisiae* culture conditions.** The culture conditions were routinely followed as reported previously (28).

**DNA amplification.** All of the DNA amplification reactions were carried out under the following temperature conditions using high-fidelity Expand (Roche) or Phusion (Finnzyme) DNA polymerases: denaturation at 94°C for 30 s, annealing at 55°C for 30 s, and extension at 72°C for 1 min. The amplification cycle was repeated 25 times. The DNA sequences of the PCR-amplified fragments were confirmed by sequencing reactions performed by Microsynth (Switzerland).

\* Corresponding author. Mailing address: AstraZeneca R & D, Bellary road, Hebbal, Bangalore, India. Phone: 91 80 2362 1212. Fax: 91 80 2362 1214. E-mail: umender.sharma@astrazeneca.com.

<sup>∇</sup> Published ahead of print on 21 March 2008.

TABLE 1. Characteristics of microbial strains and plasmids used in this study

Strain or plasmid used in this study	Relevant features	Source or reference
<b>Strains</b>		
<i>E. coli</i> DH5 $\alpha$	<i>endA1 hsdR17 supE44 recA1 relA1 (lacZYA-argF)</i>	Laboratory stock
<i>E. coli</i> BL26(DE3)	F <sup>-</sup> <i>ompT hsdB lacY T7</i> RNA polymerase expression host	Laboratory stock
<i>S. cerevisiae</i> SFY526	<i>MAT<math>\alpha</math> ura3-52 his3-200 ade2-101 lys2-801 1 leu2-3 Can<sup>r</sup> gal4-542 gal80-538 gal-lacZ</i>	Clontech
<b>Plasmids</b>		
pARC499	Derivative of pGEX3X with NcoI and BglII sites	Laboratory stock
PRSETB	<i>E. coli</i> expression vector for making N-terminal His fusions	Laboratory stock
pGBT9	<i>E. coli</i> and yeast shuttle vector for making translational fusions with the binding domain of Gal4	
pGAD424	<i>E. coli</i> and yeast shuttle vector for making translational fusions with the AD of Gal4 <sup>a</sup>	Clontech
pARC8112	<i>rpoD</i> of <i>E. coli</i> cloned into the EcoRI-Sall sites of pTrc99a	1
pARC8180	GST-AsiA fusion in the yeast expression vector pSW6	29
pARC8257	pGAD424 derivative with an NcoI site	This study
pARC8336	Rsd gene behind the T7 promoter of pET11dKm	This study
pARC8337	GST-Rsd fusion in pARC499	This study
pARC8338	His <sub>6</sub> -Rsd fusion in pRSETB	This study
pARC8339	AD-Rsd fusion in pGAD424	This study
pARC8342	GST-Rsd fusion in yeast expression vector pSW6	This study

<sup>a</sup> AD, activation domain.

**Plasmid constructs.** The plasmid DNA constructs used in this study are listed in Table 1. The  $\sigma^{70}$  constructs used in yeast two-hybrid (YTH) studies have been described previously (27). The Rsd gene was amplified from *E. coli* genomic DNA, using the forward primer sequence 5'-ACTACCATGGTTAACCAGCTCGATAAC-3' and the reverse primer sequence 5'-ACTGGATCCTTAAGCAGGATGTTTGAC-3'. The amplified PCR product was cloned into the NcoI-BamHI sites of pET11dKm to obtain pARC8336. For making the glutathione S-transferase (GST)-Rsd fusion, a 0.480-kb NcoI-BamHI fragment from pARC8336 was cloned into the NcoI-BglII sites of pARC0499 to generate pARC8337. For constructing a His-Rsd fusion, an NcoI-HindIII fragment from pARC8336 was cloned into similar sites of pRSETB to obtain pARC8338. The activation domain (AD)-Rsd fusion was generated by cloning an NcoI-BamHI fragment from pARC8336 into similar sites of pARC8257 and named pARC8339. The GST-Rsd construct pARC8342, used for expression in yeast, was generated by cloning the NcoI-HindIII fragment from pARC8337 into similar sites of pARC8180.

**Analysis of growth inhibition and quantification of protein expression.** The recombinant plasmids expressing Rsd, AsiA, GST-Rsd, and GST-AsiA were transformed into *E. coli* BL26(DE3), and plated on 0 to 100  $\mu$ M isopropyl- $\beta$ -D-thiogalactopyranoside (IPTG) at 37°C, and colony formation was analyzed after 24 h. For monitoring the growth inhibition in liquid culture, the *E. coli* expressing GST-Rsd and GST-AsiA was grown at 30°C up to an optical density at 600 nm (OD<sub>600</sub>) of 0.15 and induced with 0 to 200  $\mu$ M IPTG for 3 h, and final ODs were measured. For quantitative analysis of the protein expression in *E. coli*, Western blotting analysis using anti-GST or anti-AsiA antibodies was performed. The expressed proteins were detected by chemiluminescence (Amersham) as described previously (28). The anti-AsiA, anti-GST, and secondary antibodies were diluted 1:100,000. Standard curves were generated by using increasing amounts of purified GST-AsiA and GST-Rsd, and the linear range of detection was determined. The total cytosolic protein amounts to be loaded onto the sodium dodecyl sulfate (SDS)-polyacrylamide gels were adjusted to obtain signals in the linear range (2.5 ng to 50 ng). The scanned images were subjected to densitometric analysis by Quantity One software (Bio-Rad), and the amounts were read from the standard curve.

**Purification of GST-AsiA and GST-Rsd from *S. cerevisiae*.** *S. cerevisiae* was transformed with pARC8180 or pARC8342, using lithium acetate. The transformed yeast culture was grown in YPD (yeast extract-peptone-dextrose) medium at 30°C until an OD<sub>600</sub> of 0.8 was reached and induced with 2% galactose for 20 h. The yeast culture was resuspended in phosphate-buffered saline (pH 8.0), lysed by French pressure cell, and centrifuged at 12,000  $\times$  g, and the supernatant fraction was further used for purification. The expressed proteins were purified by glutathione affinity by the procedure suggested by the manufacturer (Pharmacia).

**Purification of  $\sigma^{70}$  and His-Rsd.** The  $\sigma^{70}$  of *E. coli* was purified from the inclusion bodies obtained from *E. coli* BL26(DE3) transformed with pARC8112 (1) by a modification of the procedure described by Borukhov and Goldfarb (2).

Briefly, it involved denaturation of the inclusion bodies by 6 M guanidine hydrochloride, followed by refolding of the protein by dialyzing out the guanidine hydrochloride against a buffer solution containing 50 mM Tris (pH 8.0), 150 mM NaCl, and 20% glycerol. To purify His-Rsd devoid of RNAP subunits, the recombinant plasmids expressing His-Rsd were transformed into *E. coli* BL26(DE3) grown at 37°C to an OD<sub>600</sub> of 0.6 and induced with 0.5 mM IPTG for 3 h. The cell pellets were resuspended in 50 mM Tris (pH 8.0) and 300 mM NaCl, lysed by a French Pressure cell, and centrifuged at 20,000  $\times$  g for 15 min (JA17 rotor; Beckman). The supernatant fraction obtained by centrifugation was used for the purification of His-Rsd fragments by Ni affinity chromatography under the denaturing conditions described in a Qiagen protocol. The purified protein was dialyzed against 50 mM Tris (pH 8.0) and 150 mM NaCl and stored at -70°C in the presence of 20% glycerol.

**In vitro GST and Ni<sup>2+</sup> affinity pull-down assays.** Purified  $\sigma^{70}$  (20  $\mu$ g), core RNAP (25  $\mu$ g; Epicenter Technologies), His-Rsd, or GST-Rsd (50  $\mu$ g) and GST-AsiA (50  $\mu$ g) in 50 mM Tris (pH 8.0), 150 mM NaCl, and 5% glycerol were mixed in the desired combinations in a 150- $\mu$ l reaction mixture, incubated at 30°C for 30 min, allowed to bind to a glutathione or Ni affinity matrix, and the unbound proteins were collected in the flow-through fractions. The affinity matrix was washed with the buffer, and the bound proteins were eluted with either 10 mM reduced glutathione or 250 mM imidazole. The eluted proteins were analyzed by SDS-polyacrylamide gel electrophoresis (PAGE).

**Native PAGE analysis.** In order to analyze protein-protein interactions, 2  $\mu$ g of each protein was taken in 25  $\mu$ l of buffer containing 50 mM Tris (pH 8.0), 150 mM NaCl, and 5% glycerol. The samples were incubated at 30°C for 15 min and subsequently loaded onto a native polyacrylamide gel consisting of a 7.5% resolving gel and a 4% stacking gel in 200 mM Tris (pH 8.8) and 10% glycerol. The gel was run at 50 V, using Tris-glycine buffer.

**Yeast transformation and  $\beta$ -galactosidase activity.** The procedure described previously (28) was followed.

**Quantitative analysis of  $\sigma^{70}$ -AsiA and  $\sigma^{70}$ -Rsd interaction.** Surface plasmon resonance (SPR; BIACore; Pharmacia) experiments were used for studying the kinetics of binding between full-length and truncated versions of  $\sigma^{70}$  and the two anti-sigma factors. For this purpose,  $\sigma^{70}$  and  $\sigma^{70}$ C100 (29) were immobilized on a CM 5 chip (Amersham), using channels 2 and 3, respectively, by using an amine coupling method described by the manufacturer to obtain 500 to 700 resonance units (RU). Channel 1 was used as a control for monitoring any nonspecific binding with the analytes. The analyte proteins (GST-AsiA, GST-Rsd, and GST) were dialyzed against HEPES buffer (10 mM HEPES [pH 7.5], 150 mM NaCl), and increasing concentrations of these proteins were passed over channels 1, 2, and 3. The flow rate was maintained at 20  $\mu$ l/min, and the binding was measured as a function of RU. The bound proteins were dissociated by passing HEPES buffer over the protein complexes and by subsequent washing with 0.5 M NaOH. Each binding procedure was repeated twice. BIAevaluation software was used for calculating various kinetic constants of the protein interactions.

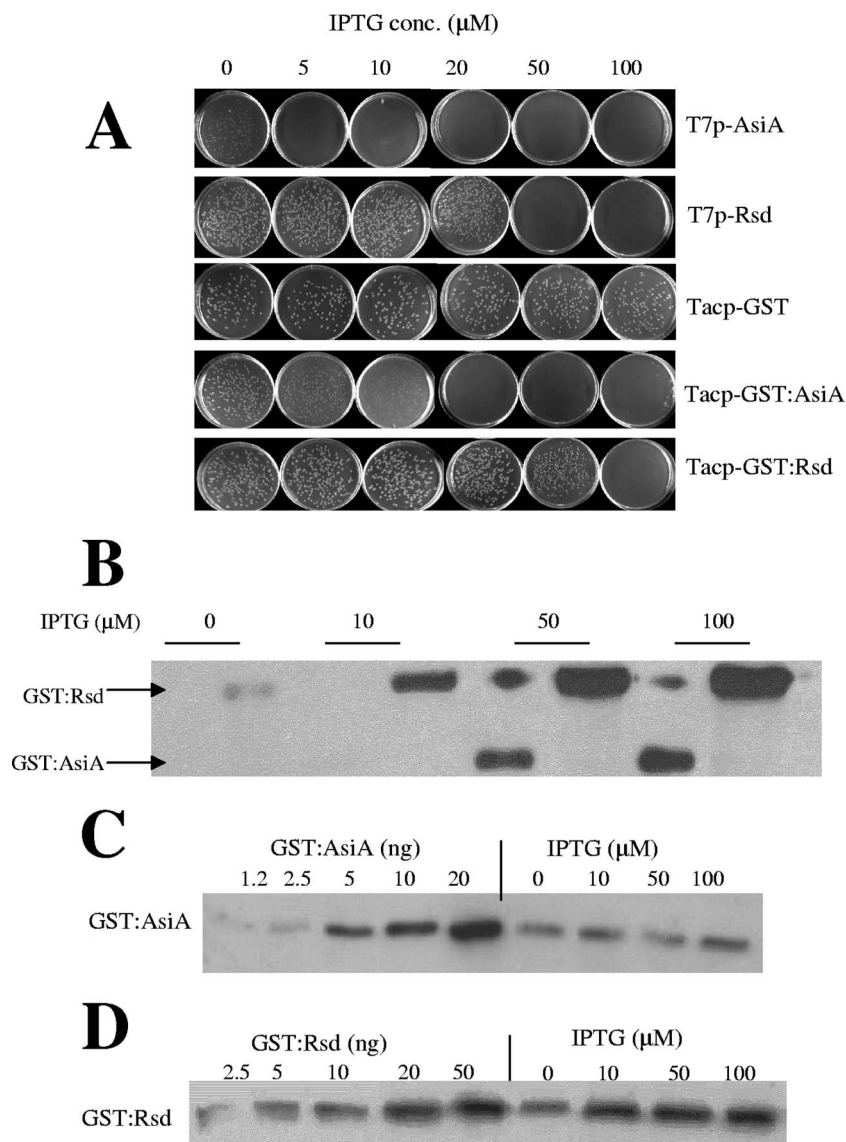


FIG. 1. Quantitative analysis of growth inhibition by T4 AsiA and *E. coli* Rsd. (A) Colony-forming abilities of *E. coli* BL26(DE3) cultures expressing AsiA, Rsd, GST, GST-AsiA, and GST-Rsd, measured in the presence of 0 to 100  $\mu\text{M}$  IPTG in agar plates; T7p, T7 promoter; Tacp, Tac promoter. Panels B, C, and D show Western blotting analyses. (B) Equal amounts (50  $\mu\text{g}$ ) of cytosolic fractions from uninduced and induced cultures of GST-AsiA and GST-Rsd were subjected to Western analysis using anti-GST antibodies. Panels C and D show quantitative Western blotting analysis of GST-AsiA and GST-Rsd expression using anti-AsiA and anti-GST antibodies, respectively. The amounts of total protein loaded were optimized to obtain signals in the linear range of standards generated from increasing amounts of purified proteins indicated in the figure.

## RESULTS

**Inhibition of *E. coli* cell growth and in vivo transcription: AsiA is more potent than Rsd.** Since it has been shown that AsiA inhibits in vitro transcription from *E. coli* promoters (21, 26) by binding to the C-terminal region of  $\sigma^{70}$ , it is fair to assume that the cellular toxicity of AsiA expression in *E. coli* (28) results from the inhibition of transcription from promoters of essential *E. coli* genes. Because Rsd is also known to bind to a similar region (region 4) of  $\sigma^{70}$  of *E. coli* (18, 26), we sought to obtain a quantitative estimate of the effect that the expression of Rsd had on in vivo transcription and growth of *E. coli*. Since overexpression of proteins in *E. coli* can cause nonspecific toxicity, we decided to follow the effects of Rsd expression on the colony-forming ability

of *E. coli* by using low concentrations (0 to 100  $\mu\text{M}$ ) of IPTG. *E. coli* BL26(DE3) cultures were individually transformed with plasmids expressing AsiA and Rsd in their native forms or as a GST fusion, and the transformed cells were plated on agar plates containing 0 to 100  $\mu\text{M}$  IPTG. As seen in Fig. 1A, the expression of Rsd or GST-Rsd did not have any effect on the colony-forming ability of *E. coli* at concentrations of 20 to 50  $\mu\text{M}$  IPTG, though AsiA- or GST-AsiA-expressing *E. coli* showed hardly any growth in the presence of 5  $\mu\text{M}$  IPTG. *E. coli* cells transformed with pGEX3x expressing GST alone could grow in the presence of 100  $\mu\text{M}$  IPTG, indicating that GST did not play any role in toxicity (Fig. 1A). Growth kinetics of the GST-AsiA and GST-Rsd fusions expressing liquid *E. coli* cultures induced with 0 to 200  $\mu\text{M}$

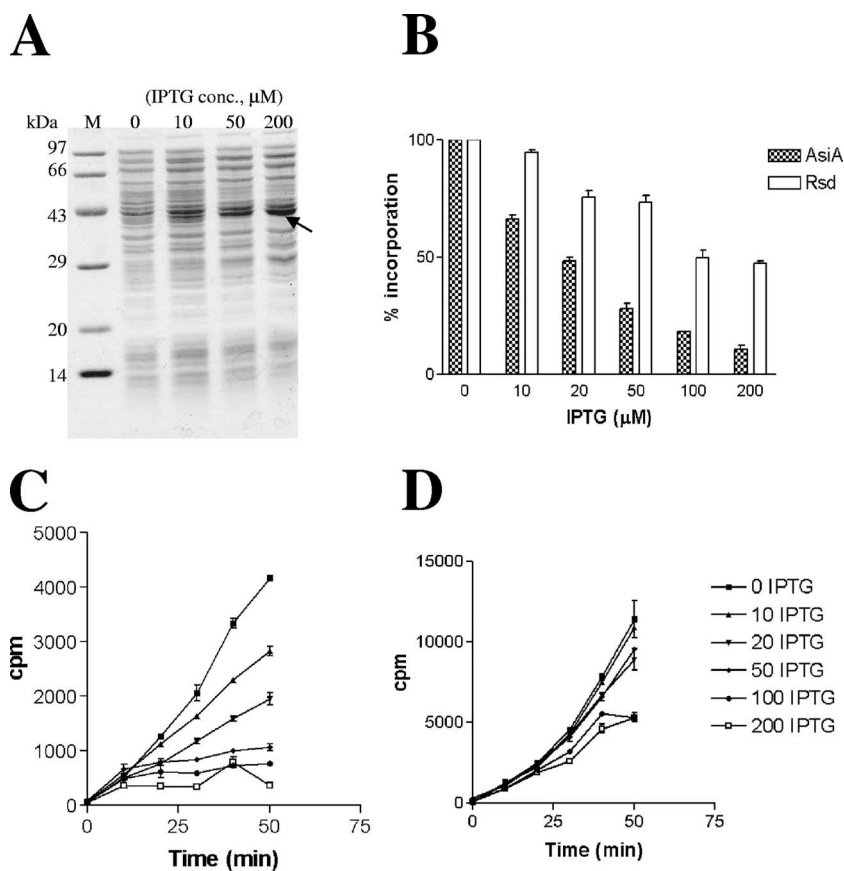


FIG. 2. Inverse correlation between protein expression and transcription inhibition by AsiA and Rsd. (A) Analysis of protein expression in cytosolic fractions of *E. coli* cultures expressing GST-Rsd, induced with 0 to 200  $\mu\text{M}$  IPTG, using Coomassie blue staining. The induced GST-Rsd band has been indicated with an arrow. Panels B to D show *in vivo* transcription inhibition by AsiA and Rsd. (B) Percentage of incorporation of [ $^3\text{H}$ ]uridine into *E. coli* cells expressing GST-AsiA or GST-Rsd after 50 min of growth in the presence of 0 to 200  $\mu\text{M}$  IPTG. Panels C and D show the incorporation of [ $^3\text{H}$ ]uridine into *E. coli* BL26(DE3) in cultures expressing GST-AsiA (C) or GST-Rsd (D) in the presence of 0 to 200  $\mu\text{M}$  IPTG, measured as trichloroacetic acid-precipitable material, as described previously (28).

IPTG showed that the GST-Rsd-expressing cultures continued growth even after 200  $\mu\text{M}$  IPTG was added (data not shown). The differences in the concentrations of IPTG required for growth inhibition in the agar plates vis-à-vis that of the liquid cultures are perhaps due to the presence of higher cell numbers in the liquid cultures ( $10^8$  CFU/ml) than in the transformed cells grown on agar plates ( $10^4$  CFU/ml).

In order to ensure that the lower level of toxicity of the Rsd was not because of lower expression levels of the protein, the expression levels of GST-Rsd and GST-AsiA in *E. coli* cultures were monitored by SDS-PAGE and Western blotting analysis. As shown earlier (28), there was no induced protein band in either the GST-AsiA-expressing or the AsiA-expressing cells, whereas an induced protein band corresponding to the expected size of the GST-Rsd fusion (43 kDa) was clearly visible in samples from *E. coli* cells expressing these proteins (Fig. 2A), indicating that the expression of Rsd is tolerated better than that of AsiA. These results also indicated that GST does not interfere with the growth-inhibiting properties of AsiA and Rsd. The exact amounts of expressed proteins were determined by quantitative Western blotting analysis. To start with, equal amounts (50  $\mu\text{g}$ ) of cytosolic proteins from cultures expressing GST-AsiA and GST-Rsd were run on SDS-PAGE,

transferred to membranes, and probed with anti-GST antibodies. As seen in Fig. 1B, under these conditions, GST-Rsd expression could be detected even in an uninduced state, whereas the expression of GST-AsiA could be seen only with cultures induced with 50  $\mu\text{M}$  IPTG, showing again the higher expression level of GST-Rsd. The quantification of the GST-AsiA and GST-Rsd expression levels was performed by densitometric analysis of the signals obtained on Western blots, as described in Materials and Methods. For this purpose, standard curves were generated by using purified GST-Rsd and GST-AsiA proteins, which were probed with anti-GST and anti-AsiA antibodies, respectively. It was found that 2.5 to 50 ng of the proteins fell in a linear range (Fig. 1C and D). The amounts of total cytosolic proteins from the GST-AsiA-expressing and GST-Rsd-expressing cultures were adjusted to obtain the signals within the linear range, and protein amounts were calculated from the reference standards. The amounts of proteins detected (percentages of the total) and the calculated intracellular concentrations of GST-AsiA and GST-Rsd are mentioned in Table 2. The concentrations of the expressed proteins were found to range from 0.11  $\mu\text{M}$  to 1.8  $\mu\text{M}$  for GST-AsiA and from 0.66  $\mu\text{M}$  to 28.90  $\mu\text{M}$  for GST-Rsd when induced in the presence of 10 to 100  $\mu\text{M}$  IPTG. It is clear that under

TABLE 2. Quantitative analysis of GST-AsiA and GST-Rsd expression in *E. coli*

Analyte	IPTG concn ( $\mu\text{M}$ )	% of total	Intracellular concn ( $\mu\text{M}$ ) <sup>a</sup>
GST-AsiA	0	0.006	0.11
	10	0.012	0.21
	50	0.062	1.1
	100	0.097	1.8
GST-Rsd	0	0.044	0.66
	10	0.307	4.6
	50	1.13	17.4
	100	1.89	28.9

<sup>a</sup> The total cytosolic protein concentration considered for the purpose of calculating GST-AsiA and GST-Rsd concentrations is 67.5 mg/ml, which is half of the total intracellular protein concentration (135 mg/ml; NEB catalogue).

inducing conditions, the level of expression of GST-Rsd was at least 15 times higher than that of GST-AsiA.

In order to compare the abilities of AsiA and Rsd to inhibit *in vivo* transcription, the incorporation of [<sup>3</sup>H]uridine in *E. coli* cells expressing GST-Rsd was measured in cells grown in the presence of 0 to 200  $\mu\text{M}$  IPTG for 50 min by the method described previously (28). Though the IPTG inductions of GST-AsiA- and GST-Rsd-expressing *E. coli* were initiated at the same cell density, the overall incorporation of radioactivity into GST-AsiA-expressing cells was found to be low, which is perhaps because of the slower growth rate caused by leaky protein expression in uninduced cells. As seen in Fig. 2C and D, there was no inhibition of [<sup>3</sup>H]uridine incorporation at 10  $\mu\text{M}$  IPTG in *E. coli* cells expressing GST-Rsd, unlike that of GST-AsiA-expressing cells, which showed an appreciable inhibition. After 50 min at 200  $\mu\text{M}$  IPTG, GST-AsiA-expressing cells showed 91.2% inhibition of incorporation as opposed to 53% in the case of GST-Rsd-expressing cells (Fig. 2B), suggesting that AsiA is a more potent inhibitor of *in vivo* transcription than Rsd. Thus, there was a good correlation between growth inhibitory properties and the ability to inhibit the incorporation of [<sup>3</sup>H]uridine into *E. coli* cells by GST-AsiA and GST-Rsd. The 50% transcription inhibitory concentrations of intracellular GST-AsiA and GST-Rsd were calculated to be approximately 0.5  $\mu\text{M}$  and 20  $\mu\text{M}$ , respectively.

**Binding affinities of AsiA and Rsd to  $\sigma^{70}$ .** We then asked whether the higher affinity of the AsiA- $\sigma^{70}$  interaction is responsible for the potent inhibitory nature of AsiA. In order to answer this question, we studied the kinetics of association and dissociation of  $\sigma^{70}$  and  $\sigma^{70}\text{C100}$  (residues 514 to 613) with GST-AsiA or GST-Rsd by SPR experiments. Since the extents of toxicity of AsiA and Rsd due to their expression and *in vitro* binding properties (see below) in their native forms and as GST fusions were found to be similar, we concluded that the GST fusion does not interfere with the binding of either of these proteins with  $\sigma^{70}$ . Thus, these proteins were purified and used as GST fusions for measuring their affinities to  $\sigma^{70}$ . For this purpose,  $\sigma^{70}$  was immobilized on a CM5 chip, and increasing concentrations of GST-AsiA, GST-Rsd, or native GST were used as analytes. The concentrations of the proteins varied from 44 nM to 2.2  $\mu\text{M}$  for GST-AsiA and from 47 nM to 2.3  $\mu\text{M}$  for GST-Rsd. There was a significant increase in RU upon increases in the concentrations of both the analyte proteins, indicating interaction with the immobilized sigma factor.

TABLE 3. Measurement of kinetic and equilibrium constant values by SPR<sup>a</sup>

Analyte	Kinetic and equilibrium values					
	$\sigma^{70}$			$\sigma^{70}\text{C100}$		
	$k_{\text{on}}$ ( $10^4$ $\text{M}^{-1} \text{s}^{-1}$ )	$k_{\text{off}}$ ( $10^{-3} \text{s}^{-1}$ )	$K_d$ (nM)	$k_{\text{on}}$ ( $10^4$ $\text{M}^{-1} \text{s}^{-1}$ )	$k_{\text{off}}$ ( $10^{-3} \text{s}^{-1}$ )	$K_d$ (nM)
GST-AsiA	2.1	1.4	67	12.7	2.0	16
GST-Rsd	4.4	1.4	32	2.9	1.7	59

<sup>a</sup> Measurements of kinetic and equilibrium constant values are from SPR experiments using  $\sigma^{70}$  and  $\sigma^{70}\text{C100}$  as the immobilized ligands and the anti-sigma factors as the analytes.  $K_d$ , dissociation constant;  $k_{\text{on}}$  and  $k_{\text{off}}$ , association and dissociation constants, respectively.

The GST fusion alone did not show any significant increase in RU, even when it was used at a concentration as high as 10  $\mu\text{M}$  (data not shown). The values of various kinetic and equilibrium constants obtained are shown in Table 3. The apparent dissociation constants ( $K_d$ ) for binding of GST-AsiA and GST-Rsd to  $\sigma^{70}$  were found to be 67 nM and 32 nM, respectively. The corresponding values for the interaction with  $\sigma^{70}\text{C100}$  were 16 nM and 59 nM, respectively. These values are in ranges similar to those reported earlier for *Bacillus subtilis* anti-sigma-sigma interactions (10, 31) but are higher than those reported for *Salmonella enterica* serovar Typhimurium FlgM- $\sigma^{28}$  interactions (7). We were tempted to conclude from the SPR experiments that the poor transcription inhibitory property of Rsd is not due to its lower affinity to  $\sigma^{70}$ .

**Rsd lacks the ability to form a stable complex with holo RNAP *in vivo* and *in vitro*.** As the differences in the inhibitory activities of AsiA and Rsd were not reflected in their binding affinities, we looked at the mechanism by which these anti-sigma factors bound to RNAP as the possible explanation for differential inhibitory properties. For this purpose, we analyzed the abilities of AsiA and Rsd to interact with  $\sigma^{70}$  and holo RNAP by analyzing *in vivo* complex formation in *E. coli* as well as *in vitro* by pull-down assays and native PAGE analysis. As shown earlier (28), the affinity-purified GST-AsiA from *E. coli* cells was found to be associated with  $\sigma^{70}$  and core RNAP subunits, demonstrating the formation of a GST-AsiA- $\sigma^{70}$ -core RNAP ternary complex (Fig. 3B, lane 2). However affinity-purified GST-Rsd purified from *E. coli* grown and induced during the log or the stationary phase ( $\text{OD}_{600}$ , 2.0) showed that  $\sigma^{70}$  was copurifying with GST-Rsd, while subunits of core RNAP were not seen (Fig. 3A). In order to detect any low-affinity interaction between GST-Rsd and RNAP, *in vivo* complex formation was studied in the presence of low salt (25 and 50 mM NaCl). No core RNAP subunits were detected under these conditions also (Fig. 3C). This indicated that either Rsd binds to free sigma only or that by binding to  $\sigma^{70}$ , it prevents its association with core RNAP.

GST-AsiA or GST-Rsd purified from *S. cerevisiae* and His-Rsd purified from *E. coli* under denaturing conditions were found to be free of any detectable RNAP subunits and, thus, were used for *in vitro* binding experiments. In order to simulate *in vivo* conditions, we used a molar excess of  $\sigma^{70}$  over that of the core RNAP (13), thus ensuring the presence of both free  $\sigma^{70}$  and holo RNAP, which was confirmed by native PAGE (see below). Furthermore, concentrations of GST-AsiA and

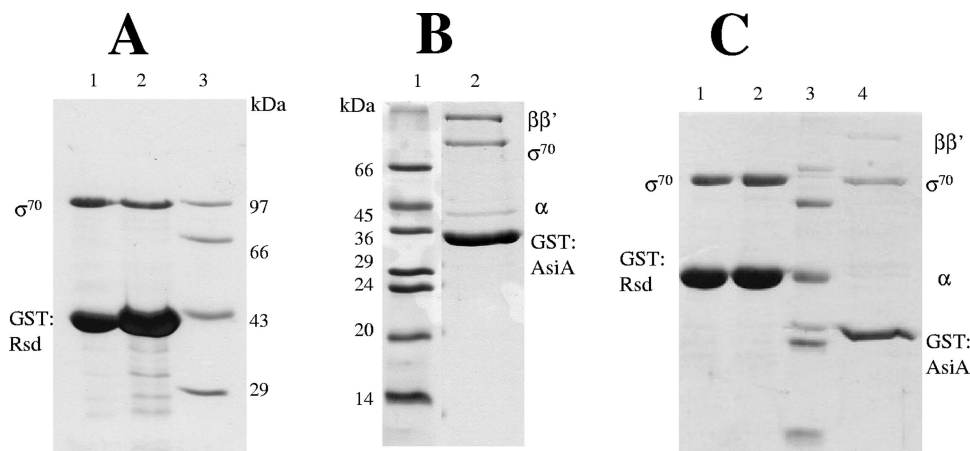


FIG. 3. Interaction between AsiA or Rsd and RNAP subunits in vivo, analyzed by coexpression and affinity purification. (A) GST-Rsd. Lanes: 1, affinity-purified GST-Rsd from log phase ( $OD_{600}$ , 0.6) culture; 2, GST-Rsd purified from stationary phase ( $OD_{600}$ , 2.5) culture; 3, molecular size marker in kDa. (B) GST-AsiA. Lanes: 1, molecular size marker (kDa); 2, affinity-purified GST-AsiA. (C) In vivo complex formation between RNAP and GST-Rsd or GST-AsiA in the presence of various concentrations of salt. Lanes: 1 and 2, GST-Rsd affinity purified in the presence of 25 mM and 50 mM NaCl, respectively; 3, molecular size marker (kDa); 4, GST-AsiA affinity purified in the presence of 500 mM NaCl.

His-Rsd were in excess of those of core RNAP and  $\sigma^{70}$ , which provided an opportunity for both free  $\sigma^{70}$  and holo RNAP to interact with these anti-sigma factors. It can be seen in Fig. 4A that GST-AsiA was able to interact with  $\sigma^{70}$  bound to core RNAP, resulting in the ternary complex formation. Similarly, an analysis of the interaction of  $\sigma^{70}$  and GST-AsiA by native PAGE showed the formation of a retarded and broad protein band (Fig. 5A, lane 5). Alteration in the mobility of a protein band upon interaction with another protein is a reliable indication of a stable complex formation, and this has also been demonstrated for a number of sigma-anti-sigma interactions (7, 10, 21). The formation of holo RNAP from  $\sigma^{70}$  and core RNAP can be visualized as a sharp band in native PAGE (Fig. 5A and B, lane 4). Upon the addition of GST-AsiA to holo RNAP, a new retarded protein band appears, and the holo RNAP band disappears completely (Fig. 5A, lane 7). Rsd was

able to bind to  $\sigma^{70}$ , and thus, the mobility of His-Rsd, as shown in native PAGE, was altered (Fig. 5B, lane 6). There was no change in the mobility of the holo RNAP band upon the addition of His-Rsd, indicating a lack of association between these proteins (Fig. 5B lane 7). However, SDS-PAGE analysis of the holo RNAP band from native PAGE showed the presence of a small amount of His-Rsd associated with holo RNAP (data not shown), thus confirming the observation made by Ilag et al. (16). The preincubation of core RNAP or  $\sigma^{70}$  with a molar excess of His-Rsd resulted in the formation of holo RNAP, and there was no indication of a ternary complex formation (data not shown). Additionally, in a pull-down experiment using increasing concentrations of His-Rsd with preincubated  $\sigma^{70}$  and core RNAP, the eluate fractions showed a linear increase in the amounts of  $\sigma^{70}$  associated with His-Rsd, but no core RNAP subunits were seen, even at the highest

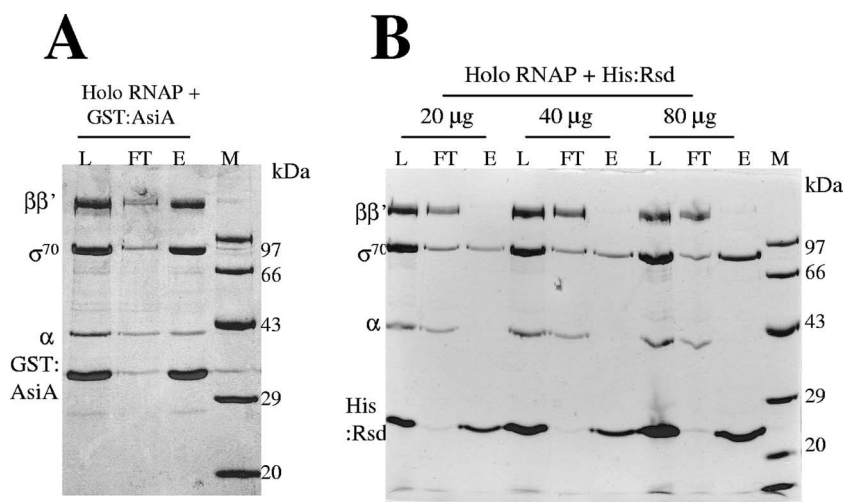


FIG. 4. In vitro interaction between AsiA or Rsd and RNAP subunits analyzed by pull-down assays. (A) Binding of GST-AsiA to holo RNAP. (B) Binding of increasing amounts of His-Rsd (20, 40, and 80  $\mu$ g) to constant amounts of holo RNAP. Load (L), flow-through (FT), and eluate (E) fractions are indicated. M, molecular size markers (kDa).

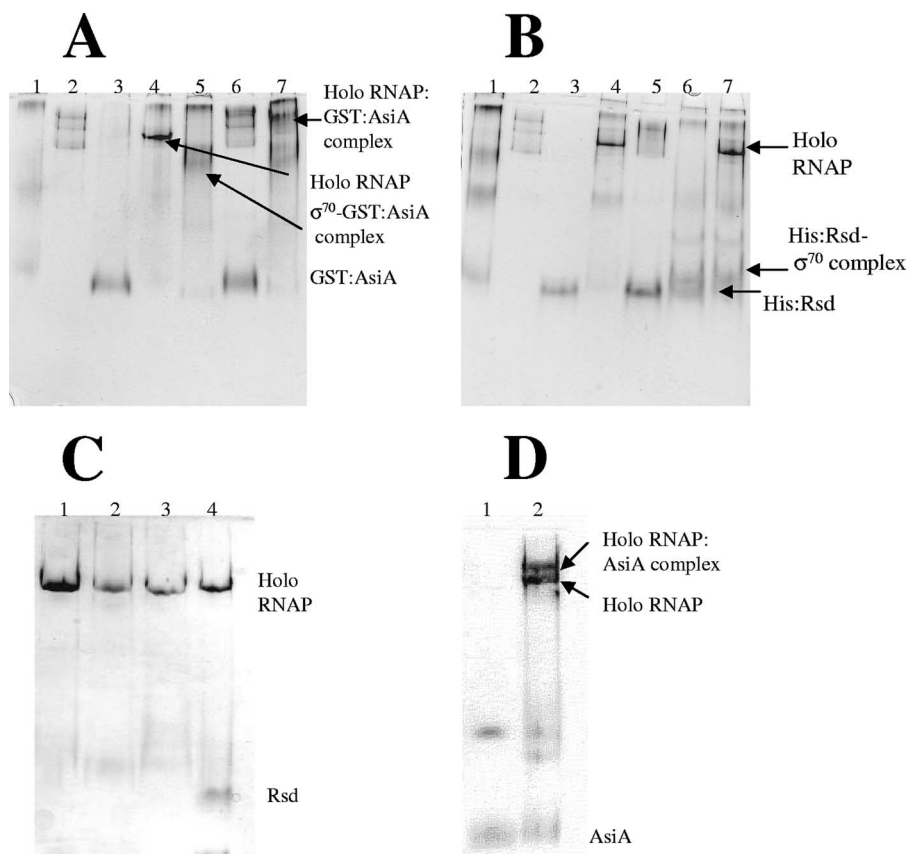


FIG. 5. In vitro interaction between AsiA or Rsd and RNAP subunits analyzed by native PAGE. (A) Lanes: 1,  $\sigma^{70}$ ; 2, core RNAP; 3, GST:AsiA; 4,  $\sigma^{70}$  plus core RNAP; 5, GST:AsiA plus  $\sigma^{70}$ ; 6, GST:AsiA plus core RNAP; 7, GST:AsiA plus holo RNAP. (B) Lanes: 1,  $\sigma^{70}$ ; 2, core RNAP; 3, His-Rsd; 4,  $\sigma^{70}$  plus core RNAP; 5, His-Rsd plus core RNAP; 6, His-Rsd plus  $\sigma^{70}$ ; 7, His-Rsd plus holo RNAP. (C) Lanes: 1,  $\sigma^{70}$  plus core RNAP; 2, GST-Rsd plus holo RNAP; 3, His-Rsd plus holo RNAP; 4, Rsd plus holo RNAP. (D) Lanes: 1, AsiA; 2, AsiA plus holo RNAP.

concentrations of His-Rsd (Fig. 4B). This again demonstrated that Rsd interacts with free  $\sigma^{70}$  but is unable to form a ternary complex with holo RNAP. In order to rule out the possibility that the affinity tags (His or GST) were interfering in the interaction of Rsd to RNAP, we generated native Rsd by cleaving GST-Rsd with factor Xa and removing GST by binding to the glutathione affinity matrix. The native Rsd also did not alter the mobility of holo RNAP in native PAGE (Fig. 5C, lane 4). However, native AsiA generated in a similar fashion retarded the holo RNAP band in nondenaturing PAGE (Fig. 5D, lane 2). Binding of either AsiA or Rsd to holo RNAP would not result in a change of pI (remains at 5.2); hence, an increase in mass upon complex formation would result in a slower moving band, as could be seen in the case of the AsiA-RNAP complex. These experiments demonstrated that the affinity tags do not interfere with the binding of Rsd or AsiA to RNAP. Thus, the major difference between the mechanisms of binding of AsiA and Rsd to RNAP is the ability of AsiA to form a stable ternary complex with RNAP.

**The binding surface of Rsd on  $\sigma^{70}$  is larger than that of AsiA.** Since the mechanisms of binding of Rsd and AsiA to RNAP were found to be different, we speculated that these proteins may be exerting differential effects on RNAP by interacting with specific regions of  $\sigma^{70}$ . Hence, we sought to

analyze this interaction in detail by trying to identify the critical region of  $\sigma^{70}$  required for binding to either of these anti-sigma factors. We had earlier identified the regions of  $\sigma^{70}$  required for interaction with AsiA, using a YTH system (27). Using the same approach, we carried out a comparative analysis of the binding of AsiA and that of Rsd to full-length and truncated forms of  $\sigma^{70}$ . As shown in Fig. 6A, in the case of Rsd, the maximum  $\beta$ -galactosidase ( $\beta$ -gal) activity was obtained with full-length  $\sigma^{70}$ , and there was a gradual decline in activity when N-terminal regions of  $\sigma^{70}$  were progressively deleted, compared to AsiA, which showed maximum  $\beta$ -gal activity with  $\sigma^{70}$  fragments lacking N-terminal regions (domains 1 and 2). The minimum region of  $\sigma^{70}$  that showed interaction with Rsd consisted of the C-terminal amino acid residues 537 to 613. Though this fragment of  $\sigma^{70}$  binds Rsd with an affinity that is lower than that of the full-length  $\sigma^{70}$ , the C-terminal region seems to be contributing the most toward this interaction, since none of the N-terminal fragments showed any  $\beta$ -gal activity in the absence of C-terminal amino acid residues 537 to 613 (data not shown). Although Rsd showed more  $\beta$ -gal activity upon interaction with full-length  $\sigma^{70}$  compared to that of AsiA, the same protein showed 200 times less activity than that of AsiA when a truncated  $\sigma^{70}$  fragment ( $\sigma^{70}$ C67, residues 547 to 613) was used.  $\sigma^{70}$  fragments lacking a part of region 4.1 (residues

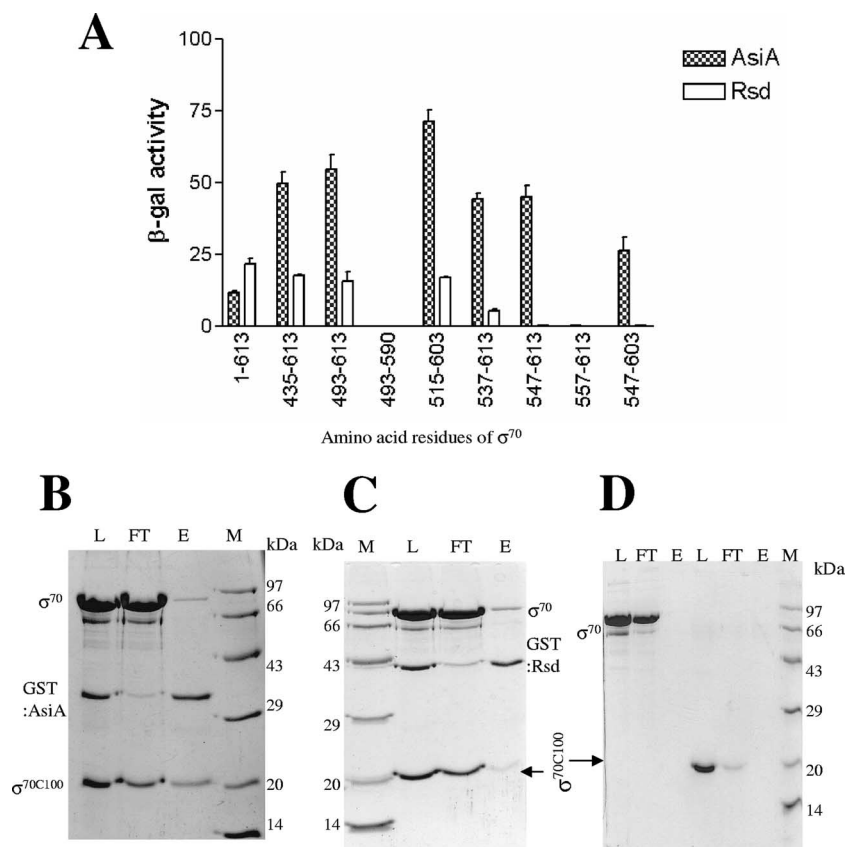


FIG. 6. Interaction of AsiA and Rsd with full-length and truncated  $\sigma^{70}$  fragments. (A) Interaction in YTH system.  $\beta$ -Gal activities of *S. cerevisiae* SFY 526 cultures carrying plasmids coding for BD- $\sigma^{70}$  variants and either AD-AsiA or AD-Rsd were assayed by using Miller's method (20). Panels B to D show analyses of the interactions of full-length and truncated  $\sigma^{70}$  fragments with GST-AsiA or GST-Rsd by using competitive binding in pull-down assays. A fourfold molar excess of full-length and truncated  $\sigma^{70}$  was mixed with GST-AsiA or His-Rsd and subjected to pull-down assays. (B) GST-AsiA plus  $\sigma^{70}$  plus  $\sigma^{70}$ C100; (C) GST-Rsd plus  $\sigma^{70}$  plus  $\sigma^{70}$ C100; (D)  $\sigma^{70}$  alone and  $\sigma^{70}$ C100 alone. Load (L), flow-through (FT), and eluate (E) fractions are shown. M, molecular size markers (kDa).

557 to 613) or 4.2 (residues 493 to 590) did not show any detectable  $\beta$ -gal activity, either with Rsd or with AsiA. Thus, amino acid residues in region 4 of  $\sigma^{70}$  make critical contacts with both Rsd and AsiA; in the case of Rsd, other regions of  $\sigma^{70}$  also contribute toward this interaction directly or indirectly, whereas AsiA- $\sigma^{70}$  interaction is restricted to regions 4.1 and 4.2 only.

Comparative affinities of full-length  $\sigma^{70}$  and two truncated  $\sigma^{70}$  fragments to AsiA or Rsd were also measured by competitive binding in pull-down assays. For this purpose, molar excess amounts of the competing  $\sigma^{70}$  fragments were incubated with limited amounts of either GST-AsiA or GST-Rsd, the mixtures of proteins were passed through the affinity matrix, and the eluted proteins were analyzed by SDS-PAGE. As seen in Fig. 6B and C, the truncated  $\sigma^{70}$  fragment  $\sigma^{70}$ C100, encompassing amino acid residues 514 to 613 (28), showed better binding to GST-AsiA than to full-length  $\sigma^{70}$ , whereas in the case of GST-Rsd, the binding of full-length  $\sigma^{70}$  was found to be better than that of the truncated  $\sigma^{70}$  fragments. Neither  $\sigma^{70}$  nor the  $\sigma^{70}$ C100 fragment showed any nonspecific binding to the glutathione affinity matrix (Fig. 6D, lanes 3 and 6). These experiments further confirm our earlier observations made with YTH assays.

## DISCUSSION

The expression of AsiA in *E. coli* results in the inhibition of growth and the loss of colony formation (28). Since T4 AsiA is a phage-encoded protein and is required only for the phage life cycle, killing the host cells seems to be evolutionarily justified. Rsd, on the other hand, is an *E. coli* protein, which, by binding to  $\sigma^{70}$ , facilitates the transcription of stationary-phase-associated genes (17, 22), and this is expected to be a reversible process. Hence, it is fair to assume that under normal physiological conditions, the binding of Rsd to *E. coli*  $\sigma^{70}$  would not result in cell death, which actually is the case.

Our quantitative analysis of the growth inhibitory properties of AsiA and Rsd showed that the expression of Rsd is tolerated much better than that of AsiA. Concomitant with this, AsiA's ability to inhibit in vivo transcription was found to be approximately 40 times higher than that of Rsd. The extent of transcription inhibition was reflected in the levels of AsiA and Rsd produced inside *E. coli* cells under inducing conditions. Because of the ability of AsiA to inhibit transcription strongly, initial amounts of AsiA produced inside the cell would also block its own synthesis along with that of other cellular proteins. On the other hand, Rsd's poor transcription inhibitory



ability does not interfere with cellular protein synthesis, which ensures higher levels of Rsd expression. Thus, the expression levels of these two proteins are inversely correlated with their transcription inhibitory properties. As a corollary to this, the mutants of AsiA, which do not inhibit *in vivo* transcription as efficiently, have lost the growth inhibitory properties and can be overexpressed in *E. coli* (28).

An obvious explanation for the higher toxicity of AsiA to *E. coli* cells, compared to that of Rsd, could have been the higher binding affinity to  $\sigma^{70}$ . However, our SPR data rule out this possibility as the dissociation constants of both of these proteins were found to be in similar ranges. Both AsiA and Rsd bind to  $\sigma^{70}$  with affinities that are comparable to those of known sigma-anti-sigma pairs (10, 31). Could the mechanism of binding to RNAP be the reason behind the higher transcription and growth inhibitory properties of AsiA? Published biochemical data do not provide an unambiguous picture of the mechanism of RNAP-Rsd interaction. While some studies have observed that Rsd binds to  $\sigma^{70}$  (17), others have suggested that in addition to binding to  $\sigma^{70}$ , Rsd also shows interaction with core RNAP and holo RNAP (16). Yet another study, by Pineda et al. (26), concluded that *E. coli* Rsd and AsiA share common mechanisms of binding to  $\sigma^{70}$  and RNAP and thus belong to the same family of proteins. However, the recent structural analysis of Rsd- $\sigma^{70}$  region 4 does not show a similarity between AsiA and Rsd (25).

Published reports of the cellular levels of  $\sigma^{70}$  and core RNAP indicate that  $\sigma^{70}$  is in excess over that of core RNAP (13) and that the majority of the core enzyme should exist in a complex with sigma factors, which means that anti-sigma factors have equal chances of interacting with free  $\sigma^{70}$  and holo RNAP. Analysis of the *in vivo* complex formation of AsiA clearly demonstrated that it binds to  $\sigma^{70}$  as well as to holo RNAP. However, our *in vivo* and *in vitro* binding experiments showed that Rsd interacts strongly with free  $\sigma^{70}$ , but there is no observable interaction with holo RNAP to form a ternary complex. We have ruled out the possibility that the affinity tags could be interfering with the binding of Rsd to holo RNAP. The interaction between Rsd and holo RNAP shown by Ilag et al. (16), using native PAGE, is probably indicative of a transient ternary complex formation which has also been shown for another anti-sigma factor, FlgM, which is capable of dissociating the  $\sigma^{28}$ -RNAP complex (7).

The YTH data presented here offer an explanation for the inability of Rsd to form a ternary complex with holo RNAP. From the comparison of binding patterns of AsiA and Rsd to  $\sigma^{70}$ , it is evident that region 4 of  $\sigma^{70}$  is the common region, which interacts with both of these anti-sigma factors, but, unlike those of AsiA, Rsd's interactions are not restricted to regions 4.1 and 4.2 alone. Binding affinities of C-terminal  $\sigma^{70}$  fragments to AsiA are greater than that of the full-length  $\sigma^{70}$ , probably because of the absence of region 1 in these proteins, which has been suggested to occlude C-terminal regions of  $\sigma^{70}$  (11). Since the region of interaction of Rsd with  $\sigma^{70}$  is much larger, partly inaccessible regions 4.1/4.2 may not affect this binding, and hence, Rsd shows better interaction with full-length  $\sigma^{70}$ . Taken together, these results suggest that by interacting with multiple regions on  $\sigma^{70}$ , which probably includes core binding regions, Rsd interferes with the  $\sigma^{70}$ -core RNAP interaction. The recent structural analysis of Rsd- $\sigma^{70}$  interac-

tion has also shown that Rsd occludes both DNA binding and core binding residues in region 4, thus indicating that Rsd can interfere with the binding of  $\sigma^{70}$  to core RNAP (25). A number of other anti-sigma factors are known to either prevent the binding of the sigma factor to core RNAP or to dissociate a sigma-RNAP complex (5–9, 32). A common feature of these anti-sigma factors is that they have multiple points of contact with their cognate sigma factors, including regions 2, 3, and 4, all of which are known to be involved in core binding (30). Since Rsd interacts with multiple regions on  $\sigma^{70}$ , its mechanism of binding seems to be similar to that of these other anti-sigma factors, which can result in the inhibition of the  $\sigma^{70}$ -core RNAP interaction, whereas AsiA, by interacting with only region 4, does not do so.

Thus, AsiA and Rsd, which share some common features of binding to  $\sigma^{70}$ , have evolved distinct mechanisms to suit their functional requirements under natural conditions. One of the reasons why Rsd does not inhibit *E. coli* growth is, probably, the inability to form a stable ternary complex with holo RNAP, thus maintaining a threshold level of transcription required for the survival of the organism. T4 AsiA, on the other hand, traps holo RNAP into a stable ternary complex, which is incapable of transcribing essential genes of *E. coli*.

#### ACKNOWLEDGMENTS

We thank Madhu for performing the BIAcore experiments. We are thankful to Jyothi Bhatt for providing purified *E. coli*  $\sigma^{70}$  and Sheela David for help in [<sup>3</sup>H]uridine incorporation experiments. Thanks to T. S. Balganes and Santanu Datta for critical reading of the manuscript. We also thank the anonymous reviewers for making suggestions for improving the manuscript.

#### REFERENCES

- Bhat, J., R. Rane, S. M. Solapure, D. Sarkar, U. Sharma, M. N. Harish, S. Lamb, D. Plant, P. Alcock, S. Peters, S. Barde, and R. K. Roy. 2006. High-throughput screening of RNA polymerase inhibitors using a fluorescent UTP analog. *J. Biomol. Screen* **11**:968–976.
- Borukhov, S., and A. Goldfarb. 1993. Recombinant *Escherichia coli* RNA polymerase: purification of individually overexpressed subunits and *in vitro* assembly. *Protein Expr. Purif.* **6**:503–511.
- Brody, E. N., G. A. Cassavetis, M. Ouhammouch, G. M. Sanders, and E. P. Geiduschek. 1995. Old phage, new insights: two recently recognised mechanisms of transcriptional regulation in bacteriophage T4 development. *FEMS Microbiol. Lett.* **128**:1–8.
- Brown, K. L., and K. T. Hughes. 1995. The role of anti sigma factors in gene regulation. *Mol. Microbiol.* **16**:397–404.
- Campbell, E. A., S. Masuda, J. L. Sun, O. Muzzin, C. A. Olson, S. Wang, and S. A. Darst. 2002. Crystal structure of the *Bacillus stearothermophilus* anti-sigma factor SpoIIAB with the sporulation sigma factor sigmaF. *Cell* **22**:795–807.
- Campbell, E. A., J. L. Tupy, T. M. Gruber, S. Wang, M. M. Sharp, C. A. Gross, and S. A. Darst. 2003. Crystal structure of *Escherichia coli* sigmaE with the cytoplasmic domain of its anti-sigma RseA. *Mol. Cell* **11**:1067–1078.
- Chadsey, M. S., J. E. Karlinsey, and K. T. Hughes. 1998. The flagellar anti-sigma factor FlgM actively dissociates *Salmonella typhimurium* sigma28 RNA polymerase holoenzyme. *Genes Dev.* **12**:3123–3136.
- Chadsey, M. S., and K. T. Hughes. 2001. A multipartite interaction between *Salmonella* transcription factor sigma28 and its anti-sigma factor FlgM: implications for sigma28 holoenzyme destabilization through stepwise binding. *J. Mol. Biol.* **306**:915–929.
- Decatur, A. L., and R. Losick. 1996. Three sites of contact between the *Bacillus subtilis* transcription factor sigmaF and its antisigma factor SpoIIAB. *Genes Dev.* **10**:2348–2358.
- Delumeau, O., R. J. Lewis, and M. D. Yudkin. 2002. Protein-protein interactions that regulate the energy stress activation of  $\sigma^B$  in *Bacillus subtilis*. *J. Bacteriol.* **184**:5583–5589.
- Dombroski, A. J., W. A. Walter, and C. A. Gross. 1993. Amino-terminal amino acids modulate sigma-factor DNA-binding activity. *Genes Dev.* **7**:2446–2455.
- Dove, S. L., and A. Hochschild. 2001. Bacterial two-hybrid analysis of interactions between region 4 of the  $\sigma^{70}$  subunit of RNA polymerase and the

- transcriptional regulators Rsd from *Escherichia coli* and AlgQ from *Pseudomonas aeruginosa*. *J. Bacteriol.* **183**:6413–6421.
13. Grigorova, I. L., N. J. Phleger, V. K. Mutalik, and C. A. Gross. 2006. Insights into transcriptional regulation and sigma competition from an equilibrium model of RNA polymerase binding to DNA. *Proc. Natl. Acad. Sci. USA* **103**:5332–5337.
  14. Helmann, J. D. 1999. Anti-sigma factors. *Curr. Opin. Microbiol.* **2**:135–141.
  15. Hughes, K. T., and K. Mathee. 1998. The anti-sigma factors. *Annu. Rev. Microbiol.* **52**:231–286.
  16. Ilag, L. L., L. F. Westblade, C. Deshayes, A. Kolb, S. J. Busby, and C. V. Robinson. 2004. Mass spectrometry of *Escherichia coli* RNA polymerase: interactions of the core enzyme with sigma70 and Rsd protein. *Structure* **12**:269–275.
  17. Jishage, M., and A. Ishihama. 1998. A stationary phase protein in *Escherichia coli* with binding activity to the major sigma subunit of RNA polymerase. *Proc. Natl. Acad. Sci. USA* **95**:4953–4958.
  18. Jishage, M., D. Dasgupta, and A. Ishihama. 2001. Mapping of the Rsd contact site on the  $\sigma^{70}$  subunit of *Escherichia coli* RNA polymerase. *J. Bacteriol.* **183**:2952–2956.
  19. Lambert, L. J., Y. Wei, V. Schirf, B. Demeler, and M. H. Werner. 2004. T4 AsiA blocks DNA recognition by remodeling sigma (70) region 4. *EMBO J.* **23**:2952–2962.
  20. Miller, J. 1992. A short course in bacterial genetics: a laboratory manual and handbook for *E. coli* and related bacteria. Cold Spring Harbor Laboratory Press, Cold Spring Harbor, NY.
  21. Minakhin, L., J. A. Camarero, M. Holford, C. Parker, T. W. Muir, and K. Severinov. 2001. Mapping the molecular interface between the sigma(70) subunit of *E. coli* RNA polymerase and T4 AsiA. *J. Mol. Biol.* **306**:631–642.
  22. Mitchell, J. E., T. Oshima, S. E. Piper, C. L. Webster, L. F. Westblade, G. Karimova, D. Ladant, A. Kolb, J. L. Hobman, S. J. Busby, and D. J. Lee. 2007. The *Escherichia coli* regulator of  $\sigma^{70}$  protein, Rsd, can up-regulate some stress-dependent promoters by sequestering  $\sigma^{70}$ . *J. Bacteriol.* **189**:3489–3495.
  23. Orsini, G., M. Ouhammouch, J. P. Le Caer, and E. N. Brody. 1993. The *asiA* gene of bacteriophage T4 codes for the anti- $\sigma^{70}$  protein. *J. Bacteriol.* **175**:85–93.
  24. Ouhammouch, M., K. Adelman, S. R. Harvey, G. Orsini, and E. N. Brody. 1995. Bacteriophage T4 MotA and AsiA proteins suffice to direct *E. coli* RNA polymerase to initiate transcription at T4 middle promoters. *Proc. Natl. Acad. Sci. USA* **92**:1451–1455.
  25. Patikoglou, G. A., L. F. Westblade, E. A. Campbell, V. Lamour, W. J. Lane, and S. A. Darst. 2007. Crystal structure of the *Escherichia coli* regulator of sigma(70), Rsd, in complex with sigma(70) domain 4. *J. Mol. Biol.* **372**:649–659.
  26. Pineda, M., B. D. Gregory, B. Szczypinski, K. R. Baxter, A. Hochschild, E. S. Miller, and D. M. Hinton. 2004. A family of anti-sigma70 proteins in T4-type phages and bacteria that are similar to AsiA, a transcription inhibitor and co-activator of bacteriophage T4. *J. Mol. Biol.* **344**:1183–1197.
  27. Sharma, U. K., S. Ravishankar, R. K. Shandil, P. V. K. Praveen, and T. S. Balganes. 1999. Study of the interaction between bacteriophage T4 AsiA and *Escherichia coli*  $\sigma^{70}$ , using the yeast two-hybrid system: neutralization of AsiA toxicity to *E. coli* cells by coexpression of a truncated  $\sigma^{70}$  fragment. *J. Bacteriol.* **181**:5855–5859.
  28. Sharma, U. K., P. V. K. Praveen, and T. S. Balganes. 2002. Mutational analysis of bacteriophage T4 AsiA: involvement of N- and C-terminal regions in binding to sigma 70 of *Escherichia coli* in vivo. *Gene* **295**:125–134.
  29. Sharma, U. K., and D. Chatterji. 2006. Both regions 4.1 and 4.2 of *E. coli* sigma(70) are together required for binding to bacteriophage T4 AsiA in vivo. *Gene* **376**:133–143.
  30. Sharp, M. M., C. L. Chan, C. Z. Lu, M. T. Marr, S. Nechaev, E. W. Merritt, K. Severinov, J. W. Roberts, and C. A. Gross. 1999. The interface of sigma with core RNA polymerase is extensive, conserved, and functionally specialized. *Genes Dev.* **15**:3015–3026.
  31. Shu, J. C., J. Clarkson, and M. D. Yudkin. 2004. Studies of SpoIIAB mutant proteins elucidate the mechanisms that regulate the developmental transcription factor sigmaF in *Bacillus subtilis*. *Biochem. J.* **384**:169–178.
  32. Sorenson, M. K., S. S. Ray, and S. A. Darst. 2004. Crystal structure of the flagellar sigma/anti-sigma complex sigma (28)/FlgM reveals an intact sigma factor in an inactive conformation. *Mol. Cell* **14**:127–138.
  33. Westblade, L. F., L. L. Ilag, A. K. Powell, A. Kolb, C. V. Robinson, and S. J. Busby. 2004. Studies of the *Escherichia coli* Rsd-sigma70 complex. *J. Mol. Biol.* **335**:685–692.